Mem. S.A.It. Vol. 88, 627

Memorie della

Pre-main-sequence evolution of low-mass stars and brown dwarfs with accretion

E. I. Vorobyov[1,2,3], V. Elbakyan[2], T. Hosokawa[4], Y. Sakurai[5], M. Guedel[3], and H. Yorke[6]

[1] Institute of Fluid Mechanics and Heat Transfer, TU Wien, Vienna, 1060, Austria
e-mail: eduard.vorobiev@univie.ac.at
[2] Research Institute of Physics, Southern Federal University, Stachki Ave. 194, Rostov-on-Don, 344090, Russia
[3] University of Vienna, Department of Astrophysics, Vienna, 1180, Austria
[4] Department of Physics, Kyoto University, Sakyo-ku, Kyoto, 113-0033, Japan
[5] Department of Physics, The University of Tokyo, Tokyo, 606-8502, Japan
[6] Jet Propulsion Laboratory, California Institute of Technology, Pasadena, CA 91109, USA

Abstract. The pre-main-sequence evolution of low-mass stars and brown dwarfs is studied numerically taking into account the mass accretion onto the central object. The stellar evolution was computed using the STELLAR evolution code developed by Yorke & Bodenheimer with recent modifications by Hosokawa et al. The mass accretion rates were taken from numerical hydrodynamics models of Vorobyov & Basu. We find that mass accretion can have a strong effect on the subsequent evolution of young stars and brown dwarfs. The disagreement between accreting and non-accreting models depends on the thermal efficiency of accretion. The largest mismatch is found for the cold accretion case. In the hot and hybrid accretion cases the disagreement between accreting and non-accreting models becomes less pronounced, but still remains notable for 1.0-Myr-old objects. These disagreements may lead to the wrong age estimate for objects of (sub-)solar mass when using the isochrones based on non-accreting models.

Key words. Accretion – Stars: formation – Stars: low-mass, brown dwarfs – Stars: pre-main sequence

1. Introduction

In the early embedded phase of protostellar disk evolution, the disks are often prone to gravitational instability (Vorobyov & Basu 2009b), which results in very time-dependent mass accretion histories, e.g., the episodic accretion histories repeating short accretion burst events and relatively longer quiescent phases (Vorobyov & Basu 2010, 2015; Machida et al. 2011).

Effects of such variable mass accretion are recently included in stellar evolution calculations focusing on the early (Vorobyov et al. 2016) and late evolutionary phases (e.g., Baraffe et al. 2009, 2012, 2016; Hosokawa et al. 2013). These studies present that PMS tracks can largely differ from the non-accreting tracks that have been used to estimate the stellar age spreads in young clusters. As a result, the age of the star as inferred from the non-accreting tracks can be considerably overestimated.

1.1. The thermal efficiency of accretion

During these calculations, we assume that a fraction α of the accretion energy $\epsilon G M_* \dot{M}/R_*$ is absorbed by the protostar, while a fraction $1-\alpha$ is radiated away and contributes to the accretion luminosity of the star. Here, M_* and R_* are the mass and radius of the central star. In this paper, we consider three scenarios for the thermal efficiency of accretion: (i) cold accretion with a constant $\alpha = 10^{-3}$, meaning that practically all accretion energy is radiated away and little is absorbed by the star, (ii) hot accretion with a constant $\alpha = 0.1$, and (iii) a hybrid scheme defined as follows:

$$\alpha = \begin{cases} 10^{-3}, & \text{if } \dot{M} < 10^{-7} \\ \dot{M} \times 10^4 \left[\frac{\text{yr}}{M_\odot}\right], & \text{if } 10^{-7} \le \dot{M} \le 10^{-5} \\ 0.1, & \text{if } \dot{M} > 10^{-5}. \end{cases} \quad (1)$$

where $\dot{M}$ is expressed in $M_\odot$ yr^{-1}.

2. Hybrid accretion

In this section, we present our model results for the hybrid accretion scenario, in which the value of α depends on the mass accretion rate. The computed stellar evolution sequences of the total (accretion plus photospheric) luminosity L_* vs. effective temperature $T_{\rm eff}$ for 31 models are shown with the dots in Figure 1. The zero point of the stellar age is defined as the time instance when the growing star accumulates 95% of its final mass. The green symbols mark the reference ages of 1 Myr, 10 Myr, and 25 Myr for each model. The black solid lines present the isochrones for the same ages, but derived from the non-accreting stellar evolution models of Yorke & Bodenheimer (2008) (hereafter, the non-accreting isochrones).

A visual inspection of Figure 1 indicates that young objects show a notable deviation from the non-accreting isochrones. This is especially evident for the models with effective temperatures $\log T_{\rm eff} \ge 3.5$, which lie notably lower than the 1.0-Myr-old isochrone, meaning that these objects appear older on the L_*–$T_{\rm eff}$ diagram than they truly are.

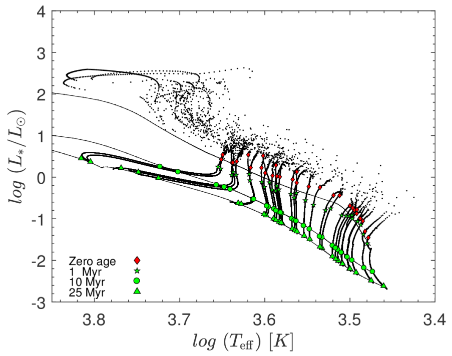

Fig. 1. Stellar evolution sequences on the total luminosity L_* – effective temperature $T_{\rm eff}$ diagram for the hybrid accretion models. The dots present the model tracks. The zero point age for each model is marked by the red diamonds. The green symbols mark the reference ages as indicated in the bottom-left corner, elapsed since the zero point age of each object. The black solid lines provide the isochrones for stellar ages of 1 Myr, 10 Myr and 25 Myr (from top to bottom) derived from non-accreting stellar evolution models of Yorke & Bodenheimer (2008).

3. Hot accretion

In this section, we present the results for the hot accretion scenario, in which α is set to 0.1 during the entire evolution period. For the models with the hot accretion scenario there again exists a moderate deviation between the accreting and non-accreting 1.0-Myr-old models in terms of the total luminosity and stellar radius, but this disagreement diminishes for 10-Myr-old and 25-Myr-old models. All in all, the behaviour of the hybrid and hot accretion models is similar, in agreement with the previous work of Baraffe et al. (2012).

4. Cold accretion

In this section, we present our results for the cold accretion scenario, in which α is always set to a small value of 10^{-3} independent of the actual value of the mass accretion rate, mean-

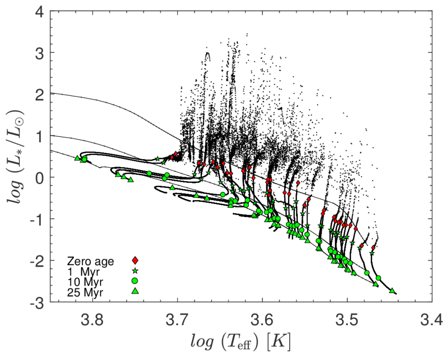

Fig. 2. Similar to Figure 1 but for the cold accretion scenario.

ing that almost all accretion energy is radiated away and only a tiny fraction is absorbed by the protostar. Figure 2 shows the stellar evolutionary sequences for all models. The meaning of the symbols and lines is the same as in Figure 1.

On average, the disagreement between the cold accretion models and the corresponding non-accreting models of Yorke & Bodenheimer has increased by about a factor of several as compared to the case of hybrid accretion. More specifically, the deviations in L_* for the 1.0-Myr-old models have grown by a factor of 2, while the deviations in $T_{\rm eff}$ and R_* have grown by factors of 3–4. The disagreement for older models is even more notable: the deviation in L_* for the 10-Myr-old objects has increased on average by a factor of 4 and may reach as much as a factor of 10 for some upper mass models. The same tendency is found for the stellar radius.

5. Conclusions

Our key findings can be summarized as follows.

- In the hybrid accretion case, young 1.0-Myr-old objects show notable deviations from the non-accreting isochrones and isomasses for both low-mass stars and brown dwarfs.
- The hot accretion case is qualitatively similar to hybrid accretion, but showing somewhat smaller deviations for L_* and R_*.
- The cold accretion case features the largest deviations from the non-accreting models of Yorke & Bodenheimer.
- As a result of this mismatch, the use of the L_*–$T_{\rm eff}$ diagram may lead to the false age estimate for objects with $T_{\rm eff} > 3500$ K, as was also previously noted in Baraffe et al. (2009) and Hosokawa et al. (2011).

Acknowledgements. This project was supported by the Russian Ministry of Education and Science Grant 3.961.2014/K. V.G.E. acknowledges The Southern Federal University for financial support for international research. The simulations were performed on the Vienna Scientific Cluster (VSC-2 and VSC-3) and on the Shared Hierarchical Academic Research Computing Network (SHARCNET).

References

Baraffe, I., Chabrier, G., & Gallardo, J. 2009, ApJ, 702, L27
Baraffe, I., Vorobyov, E. I., & Chabrier, G. 2012, ApJ, 756, 118
Baraffe, I., et al. 2016, A&A, in press
Hosokawa, T., Offner, S., & Krumholz, M. 2011, ApJ, 738, 140
Hosokawa, T., Yorke, H., Inayoshi, K. et al. 2013, ApJ, 778, 178
Machida, M. N., Inutsuka, S., & Matsumoto, T. 2011, ApJ, 729, 42
Vorobyov, E. I., & Basu, S. 2009, MNRAS, 393, 822
Vorobyov, E. I., & Basu, S. 2010, ApJ, 719, 1896
Vorobyov, E. I., & Basu, S. 2015, ApJ, 805, 115
Vorobyov, E. I., et al. 2016, A&A, `arXiv161203696V`, in press
Yorke H. W., & Bodenheimer P. 2008, in Massive Star Formation: Observations Confront Theory, Beuther H., Linz H., Henning T., eds. (ASP, San Francisco), ASP Conf. Ser., 387, 189